Proc. of JSCE,
No. 185, Jan. 1971

A VISCOELASTIC APPROACH TO THE PROBLEM OF STRESS WAVE PROPAGATION IN COHESIVE SOILS*

*By Koichi AKAI** and Masayuki HORI****

1. INTRODUCTION

During an earthquake a large amount of energy propagates through earth ground from deep bed rock upward to the ground surface. On the other hand, vibrations and impacts caused by traffic facilities or construction machineries on the ground surface transmit their energy into ground. Just contrarily to that the main motion of the former consists of shear waves, dilatational waves constitute main parts in the latter case. In spite of such a difference, however, both phenomena occur with very short duration of time.

When investigating the soil behavior constituting earth ground, we have to make it possible to know not only the long-term characteristics such as creep or stress relaxation but the above-mentioned various dynamic phenomena. The authors treat the propagation of stress wave in soil media as an approach to soil dynamics problems. For simplicity only one-dimensional problems are considered here.

Generally speaking, during the propagation process of stress waves in soil the energy is absorpted by compaction (*i.e.*, intergranular friction) and viscosity of soil materials. The damping effect of energy differs by the kind of soil.

We have recongnized some remarkable phenomena in the one-dimensional longitudinal impact test for cohesive soils as follows :

1) Finite velocity of wave front,
2) Attenuation of peak stress with distance,
3) Increase in rise time with distance,
4) Increase in duration time with distance, and
5) Time lag in displacement.

One can express the above phenomena by the term of "collapse of wave" which is a measure of energy damping characteristics of soil. For theoretical analysis of the damping characteristics due to viscosity, it is usual to assume the viscoelastic damping mechanism[1]. Assuming semi-infinite one-dimensional rods of some linear viscoelastic models, in the present paper, theoretical solutions are obtained for the stress propagation problems in the case of boundary stress forming a spike pulse with exponential decay.

2. PREVIOUS STUDIES

Lee and Kanter[2] mainly concerned with a Maxwell material, which corresponds to a model having a spring and a dashpot in series. The equation for longitudinal wave propagation in rods is shown to be equivalent to the telegraph equation, and solutions of transient wave problems were treated briefly using the Laplace transform technique. Impact on a semi-infinite rod was considered as step pulse in detail and a method of superposition of image was discussed to use this solution to solve boundary value problems for finite rods. The resulting stress distributions were discussed and contrasted with those for an elastic rod.

Transient wave analysis in a linear time-dependent material was performed by Glauz and Lee[3]. They considered a body which exhibits an elastic, viscous, or retarded elastic response under stress. For the particular case of a constant velocity applied at the end of a semi-infinite bar, the transient stresses, strains and velocities were found by the method of characteristics. From this solution they obtained the stresses for the case of a constant stress applied at the end of a semi-infinite bar. By superposition can also be solved problems of finite bars, and for a constant velocity applied at the end of the bar an integral expression was derived for the stress at that end as a function of time.

The stress and velocity distributions associated with the propagation of an impulsively applied velocity and stress along rods of viscoelastic materials

---

* Presented at the 25th Annual Meeting of J.S.C.E., Nov., 1970

** Dr. Eng., Professor of Civil Engineering, Kyoto University

*** Graduate course student, Kyoto University

were throughly analyzed by Morrison[4] and by Lee and Morrison[5]. Various viscoelastic materials were considered of complexity from the simple Voigt and Maxwell model up to that represented by a four-element model which exhibits a combination of instantaneous elastic response, and permanent viscous flow. The stress distribution for both cases of constant applied stress and constant applied velocity was represented graphically for the materials considered, dimensionless coordinates being used.

Propagation of stress pulses in standard linear viscoelastic models was also treated by Lai and Sauer[6]. In this study, the transient stress, strain, and particle velocity responses of a semi-infinite rod for boundary stress either applied impulsively and subsequently maintained constant or characteristic of airblast from nuclear and high explosive detonations were numerically determined. The results for the step-function-stress boundary condition were in excellent agreement with previous results found by Laplace transform methods and extended the useful range in time and depth of the solution by more than threehold. For the airblast-loading boundary condition it was found that for large yield detonations (long overpressure pulses) the attenuation with depth of maximum responses was small and hence the medium behaves quasi-elastically, while spike pulses characteristic of high explosive detonations gave rise to more nearly viscoelastic behavior.

Seaman[7] studied soil behavior during stress wave propagation on a sand and two clays by making one-dimensional wave propagation tests of five-meter long columns of the soils. Attempts were made to predict this behavior by determining soil properties in dynamic compression tests on small samples and by using these properties in a variety of mathematical models for soil. Two theoretical soil models were analyzed in this study; one to investigate the effect of combined time-dependent and time-independent dissipation and another to study the effects of nonlinear stress-strain relations and geostatic stress. They were termed as viscoelastic compacting model and S-hysteretic model, respectively. A comparison of wave propagation results and of theoretical predictions based on compression test properties showed that the arrival time of the stress wave could be predicted from the compression modulus of the soil, and that the stress attenuation could be predicted from the dissipative soil parameters found in the compression tests.

3. THEORETICAL MODELS

(1) General

Morrison[4] obtained theoretical solutions for stress distribution in various linear viscoelastic one-dimensional rods, giving the boundary stress of step-pulse type. The attenuation of peak stress in soil depends upon the wave form of pulsative stress given at the surface as well as the wave propagation velocity. In the previous works that we have ever performed, the surface stress obtained by the drop hammer is of spike-pulse type which reaches the peak stress linearly within the rise time of about 2~5 msec and decreases exponentially thereafter[8),9)].

In order to perform comparison with experimental results and also generalization of surface stresses, we consider a boundary stress exhibiting a shock front behind which it attenuates with a constant parameter. The solutions for stress propagation in one-dimensional rods of Voigt model and Maxwell model are obtained by means of Laplace transform as follows.

(2) Voigt model

We are concerned with a semi-infinite rod, $x \geq 0$, of Voigt-type viscoelastic material where the x-coordinate is measured along the length of the rod. The equation of motion is

$$\rho u_{tt} = -\sigma_x \quad \cdots\cdots(1)$$

where ρ denotes the density of the unstrained material, $u(x, t)$ the displacement in the direction of x, $\sigma(x, t)$ the nominal compression stress, *i.e.*, the force per unit initial cross-sectional area transmitted across the section x of the rod and the subscripts represent partial differentiation with respect to the corresponding variable.

Correlation between the nominal compressive strain $\varepsilon(x, t)$ and the displacement $u(x, t)$ is

$$\varepsilon = -u_x \quad \cdots\cdots(2)$$

The Voigt model is shown in Fig. 1 and is composed of a spring and a dashpot in parallel. The constitutive equation of this model is

$$\sigma = E\varepsilon + \frac{1}{\mu}\varepsilon_t \quad \cdots\cdots(3)$$

where E and μ are elastic and viscous constants, respectively, for the material.

Eliminating σ and ε from Eqs. (1), (2) and (3), we obtain

$$\rho u_{tt} = Eu_{xx} + \frac{1}{\mu}u_{xxt} \quad \cdots\cdots(4)$$

from which it is readily verified that the stress σ

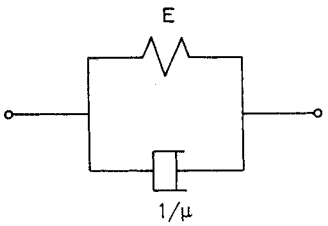

Fig. 1 Voigt model.

and the particle velocity $v=u_t$ both satisfy the partial differential equation :

$$\rho f_{tt}=Ef_{xx}+\frac{1}{\mu}f_{xxt} \quad \cdots\cdots(5)$$

We introduce the following dimensionless variables in order to facilitate inversive Laplace transformation afterwards.

$$\xi=(\rho E)^{1/2}\mu x,\ \tau=E\mu t,\ \Sigma'=\frac{\sigma(x,t)}{\sigma_0} \quad \cdots(6)$$

Then, Eq. (5) is written in the dimensionless form as :

$$\Sigma_{\tau\tau}'=\Sigma_{\xi\xi}'+\Sigma_{\xi\xi\tau}' \quad \cdots\cdots(7)$$

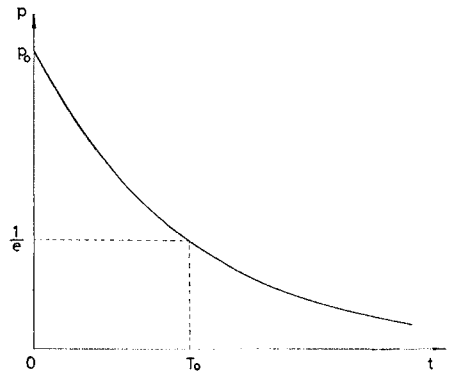

Fig. 2 Applied surface pulse.

The surface pulse is considered as follows, refering Fig. 2.

$$\frac{p}{p_0}=e^{-\alpha t}=e^{-t/T_0}=e^{-\tau/E\mu T_0}=e^{-\beta\tau} \quad \cdots\cdots(8)$$

where $\beta=1/E\mu T_0$ (T_0 : relaxation time). For $\beta=0$ the surface stress becomes to a step-pulse, and $\beta=\infty$ corresponds to a single pulse. Thus the boundary conditions are

$$\Sigma'(\infty,\tau)=0,\ \Sigma'(0,\tau)=e^{-\beta\tau} \quad \cdots\cdots(9)$$

Considering Laplace transformation :

$$L\{f(\xi,\tau)\}=\int_0^\infty e^{-s\tau}f(\xi,\tau)d\tau \quad \cdots\cdots(10)$$

then, Eq. (7) is reduced to the following ordinary differential equation.

$$s^2L\{\Sigma'\}=(1+s)[L\{\Sigma'\}]_{\xi\xi} \quad \cdots\cdots(11)$$

On the other hand, the transformations of the boundary conditions, Eqs. (9), are

$$L\{\Sigma'(\infty,\tau)\}=0,\ L\{\Sigma'(0,\tau)\}=\frac{1}{s+\beta} \quad \cdots(12)$$

Solving Eq. (11) under the conditions of Eqs. (12), we obtain

$$L\{\Sigma'(\xi,\tau)\}=\frac{1}{s+\beta}\exp\left\{\frac{-\xi s}{\sqrt{1+s}}\right\} \quad \cdots\cdots(13)$$

In order to obtain the inversive transformation of Eq. (13) we use the following formulae :

(a) $\frac{1}{s}\exp(-\eta s)=L\{H(\tau-\eta)\}$,

H : Heaviside step function

(b) $\exp\left(-\frac{\xi}{s}\right)=L\left\{\delta(\tau)-\left(\frac{\xi}{\tau}\right)^{1/2}J_1(2\sqrt{\xi\tau})\right\}$,

J_1 : the first kind of Bessel function of first order

(c) $\exp(-\xi\sqrt{s})=L\left\{\frac{\xi}{2\sqrt{\pi\tau^3}}\exp\left(-\frac{\xi^2}{4\tau}\right)\right\}$

From the formula (a),

$$\begin{aligned}&\frac{1}{s}\exp\{-\eta(s-\beta+1)\}\\&=\exp\{\eta(\beta-1)\}\frac{1}{s}\exp(-\eta s)\\&=\exp\{\eta(\beta-1)\}L\{H(\tau-\eta)\}\\&=L[\exp\{\eta(\beta-1)\}H(\tau-\eta)] \quad \cdots\cdots(14)\end{aligned}$$

Using the integral formula* and (b),

$$\begin{aligned}\frac{1}{s}\exp\left\{-\frac{\xi}{s-\beta+1}\right\}=L\Big[&\int_0^\infty\exp\{\eta(\beta-1)\}\\&\cdot H(\tau-\eta)\left\{\delta(\eta)-\left(\frac{\xi}{\eta}\right)^{1/2}J_1(2\sqrt{\xi\eta})\,d\eta\right\}\Big]\end{aligned} \quad \cdots\cdots(15)$$

From the shift theorem,

$$\begin{aligned}\frac{1}{s+\beta-1}\exp\left(\frac{-\xi}{s}\right)=L\Big[&\int_0^\tau\exp\{-(\beta-1)(\tau-\eta)\}\\&\cdot\left\{\delta(\eta)-\left(\frac{\xi}{\eta}\right)^{1/2}J_1(2\sqrt{\xi\eta})\,d\eta\right\}\Big]\end{aligned} \quad \cdots\cdots(16)$$

Then,

$$\begin{aligned}&\frac{1}{s+\beta-1}\exp\left\{-\eta\left(s+\frac{1}{s}-2\right)\right\}\\&=L\Big[\int_0^{\tau-\eta}\exp\{-(\beta-1)(\tau-\eta-t)\}\\&\quad\cdot\left\{\delta(t)-\left(\frac{\eta}{t}\right)^{1/2}J_1(2\sqrt{\eta t})\right\}\\&\quad\cdot\exp(2\eta)H(\tau-\eta)\,dt\Big]\\&=L\{f(\tau,\eta)H(\tau-\eta)\}\end{aligned} \quad \cdots\cdots(17)$$

From (c) and Eq. (17), using the integral formula,

$$\begin{aligned}&\frac{1}{s+\beta-1}\exp\left\{\frac{-\xi(s-1)}{\sqrt{s}}\right\}\\&=L\left\{\int_0^\tau f(\tau,\eta)\frac{\xi}{2\sqrt{\pi\eta^3}}\exp\left(-\frac{\xi^2}{4\eta}\right)d\eta\right\}\\&=L\left\{\frac{\xi}{2\sqrt{\pi}}\int_0^\tau f(\tau,\eta)\frac{1}{\sqrt{\eta^3}}\exp\left(-\frac{\xi^2}{4\eta}\right)d\eta\right\}\end{aligned} \quad \cdots\cdots(18)$$

Again from the shift theorem,

$$\begin{aligned}\frac{1}{s+\beta}\exp\left\{\frac{-\xi s}{\sqrt{1+s}}\right\}=L\Big\{&\frac{\xi\exp(-\tau)}{2\sqrt{\pi}}\\&\cdot\int_0^\tau f(\tau,\eta)\frac{1}{\sqrt{\eta^3}}\exp\left(-\frac{\xi^2}{4\eta}\right)d\eta\Big\}\end{aligned} \quad \cdots\cdots(19)$$

where,

$$\begin{aligned}f(\tau,\eta)&=\int_0^{\tau-\eta}\exp\{-(\beta-1)(\tau-\eta-t)\}\\&\quad\cdot\left\{\delta(t)-\left(\frac{\eta}{t}\right)^{1/2}J_1(2\sqrt{\eta t})\right\}\exp(2\eta)dt\\&=\exp\{2\eta-(\beta-1)(\tau-\eta)\}\\&\quad\cdot\int_0^{\tau-\eta}\left\{\delta(t)-\left(\frac{\eta}{t}\right)^{1/2}J_1(2\sqrt{\eta t})\right\}dt\\&=\exp\{2\eta-(\beta-1)(\tau-\eta)\}g(\tau,\eta)\end{aligned} \quad \cdots\cdots(20)$$

Finally we obtain the following solution.

$$\Sigma'(\xi,\tau)=\frac{\xi}{2\sqrt{\pi}}\exp(-\beta\tau)\int_0^\tau\frac{g(\tau,\eta)}{\sqrt{\eta^3}}$$

* See Appendix

$$\cdot\exp\left\{(\beta+1)\eta-\frac{\xi^2}{4\eta}\right\}d\eta \quad \cdots\cdots(21)$$

where,

$$\left.\begin{aligned} g(\tau,\eta)&=\int_0^{\tau-\eta}\left\{\delta(\zeta)-\left(\frac{\eta}{\zeta}\right)^{1/2}J_1(2\sqrt{\eta\zeta})\right\}d\zeta \\ J_1(2\sqrt{\eta t})&=\sqrt{\eta t}\sum_{m=0}^{\infty}\frac{(-1)^m(\eta t)^m}{m!\,\Gamma(m+2)} \end{aligned}\right\} \quad \cdots\cdots(21)'$$

In the special case for $\beta=1$, one obtains the following solution by using another type of transformation*.

$$\Sigma'(\xi,\tau)=\frac{e^{-\tau}}{\pi}\int_0^{\tau}\left[\frac{\cos\{2\sqrt{\eta(\tau-\eta)}\}}{\sqrt{\eta(\tau-\eta)}}-\frac{\sin\{2\sqrt{\eta(\tau-\eta)}\}}{\eta}\right]\exp\left(2\eta-\frac{\xi^2}{4\eta}\right)d\eta \quad \cdots\cdots(22)$$

The solution for a step-pulse type boundary stress which has been deduced by Morrison[4] is expressed as :

$$\Sigma'(\xi,\tau)=\frac{e^{-\tau}}{\pi}\int_0^{\tau}\frac{\cos\{2\sqrt{\eta(\tau-\eta)}\}}{\sqrt{\eta(\tau-\eta)}}\cdot\exp\left(2\eta-\frac{\xi^2}{4\eta}\right)d\eta \quad \cdots\cdots(23)$$

Comparing Eqs. (22) and (23), the difference is only the term of $\sin\{2\sqrt{\eta(\tau-\eta)}\}/\eta$ in parentheses. This means that the propagating stress attenuates more rapidly for a spike-pulse shock wave than for a step-pulse.

(3) Maxwell model

Instead of Eq. (3), we use the constitutive equation :

$$\mu\sigma+\frac{1}{E}\sigma_t=\varepsilon_t \quad \cdots\cdots(24)$$

then, the fundamental partial differential equation for Maxwell model (Fig. 3) is

$$\Sigma_{\xi\xi}'-\Sigma_{\tau\tau}'-\Sigma_{\tau}'=0 \quad \cdots\cdots(25)$$

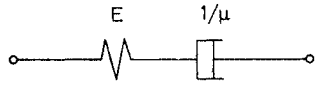

Fig. 3 Maxwell model.

By solving the equation using the same boundary conditions as Eq. (12) after Laplace transformation, one obtains the following transformed normalized stress.

$$L\{\Sigma'(\xi,\tau)\}=\frac{1}{s+\beta}\exp\{-\sqrt{s(s+1)}\xi\} \quad \cdots(26)$$

In order to make the inversive transformation of Eq. (26) we choose the following formulae :

(a) $\exp(-\xi\sqrt{s^2-a^2})-\exp(-\xi s)$

$$=L\left\{\frac{a\xi}{\sqrt{\tau^2-\xi^2}}I_1(a\sqrt{\tau^2-\xi^2})H(\tau-\xi)\right\},$$

I_1 : the first kind of modified Bessel function of first order

(b) $\frac{1}{s}\exp(-\eta s)=L\{H(\tau-\eta)\}$

From the formula (a),

$$\exp(-\xi\sqrt{s^2-a^2})=L\left\{\delta(\tau-\eta)+\frac{a\xi}{\sqrt{\tau^2-\xi^2}}\cdot I_1(a\sqrt{\tau^2-\xi^2})H(\tau-\xi)\right\} \quad \cdots\cdots(27)$$

Taking $a=1/2$,

$$\exp(-\xi\sqrt{s^2-0.25})=L\left\{\delta(\tau-\eta)+\frac{\xi}{2\sqrt{\tau^2-\xi^2}}\cdot I_1\left(\frac{1}{2}\sqrt{\tau^2-\xi^2}\right)H(\tau-\xi)\right\} \quad \cdots\cdots(28)$$

From (b),

$$\frac{1}{s}\exp\left\{-\left(s-\beta+\frac{1}{2}\right)\eta\right\}=\frac{1}{s}\exp(-\eta s)\exp\left\{\left(\beta-\frac{1}{2}\right)\eta\right\}=L\left[\exp\left\{\left(\beta-\frac{1}{2}\right)\eta\right\}H(\tau-\eta)\right] \quad \cdots\cdots(29)$$

From the shift theorem,

$$\frac{1}{s+\beta-\frac{1}{2}}\exp(-\eta s)=L\left[\exp\left\{-\left(\beta-\frac{1}{2}\right)\tau\right\}\exp\left\{\left(\beta-\frac{1}{2}\right)\eta\right\}H(\tau-\eta)\right]=L\left[\exp\left\{-\left(\beta-\frac{1}{2}\right)(\tau-\eta)\right\}H(\tau-\eta)\right] \quad \cdots\cdots(30)$$

Applying the integral formula to Eqs. (28) and (30),

$$\frac{1}{s+\beta-\frac{1}{2}}\exp(-\xi\sqrt{s^2-0.25})=L\left\{\int_0^{\tau}\exp\left\{-\left(\beta-\frac{1}{2}\right)(\tau-\eta)\right\}\cdot\left\{\delta(\eta-\xi)+\frac{\xi}{2\sqrt{\eta^2-\xi^2}}\cdot I_1\left(\frac{1}{2}\sqrt{\eta^2-\xi^2}\right)H(\tau-\eta)\right\}d\eta\right. \quad \cdots\cdots(31)$$

From the shift theorem,

$$\frac{1}{s+\beta}\exp\left\{-\sqrt{s(s+1)}\xi\right\}=L\left[\int_0^{\tau}\exp\left\{\left(\beta-\frac{1}{2}\right)\eta-\beta\tau\right\}\delta(\eta-\xi)d\eta+\int_0^{\tau}\frac{1}{2}\exp\left\{\left(\beta-\frac{1}{2}\right)\eta-\beta\tau\right\}\frac{\xi}{\sqrt{\eta^2-\xi^2}}\cdot I_1\left(\frac{1}{2}\sqrt{\eta^2-\xi^2}\right)H(\eta-\xi)d\eta\right] \quad \cdots\cdots(32)$$

As the result we obtain the following solution.

$$\Sigma'(\xi,\tau)=\exp\left\{\left(\beta-\frac{1}{2}\right)\xi-\beta\tau\right\}+\frac{1}{2}\int_{\xi}^{\tau}\exp\left\{\left(\beta-\frac{1}{2}\right)\eta-\beta\tau\right\}\frac{\xi}{\sqrt{\eta^2-\xi^2}}\cdot I_1\left(\frac{1}{2}\sqrt{\eta^2-\xi^2}\right)d\eta \quad (\tau\geq\xi)\cdots\cdots(33)$$

The solution for the boundary stress of step-pulse given by Lee and Kanter[2] is,

$$\Sigma'(\xi,\tau)=\exp\left(-\frac{1}{2}\xi\right)+\frac{1}{2}\int_{\xi}^{\tau}\exp\left(-\frac{1}{2}\eta\right)\cdot\frac{\xi}{\sqrt{\eta^2-\xi^2}}I_1\left(\frac{1}{2}\sqrt{\eta^2-\xi^2}\right)d\eta \quad (\tau\geq\xi)\cdots(34)$$

* See Appendix

Putting $\beta=0$ in Eq. (33) gives the same expression as Eq. (34).

4. CALCULATED RESULT AND DISCUSSION

(1) Voigt model

The analytical solution (22) which corresponds to the boundary stress of $\exp(-\tau)$ has been numerically integrated by means of FACOM 230-60 Digital Computer in Kyoto University, by using the Simpson's integral formula with the integral intervals of 10^{-4}. The calculated result is indicated in Fig. 4. The broken line in the figure corresponds to the boundary condition (the second equation of Eqs. (9)) originally given which should be in accordance with the curve for $\xi=0$. One notes some deviation between these curves in the figure. The reason seems to be the existence of singular points at $\eta=0$ and $\eta=\tau$ in Eq. (22).

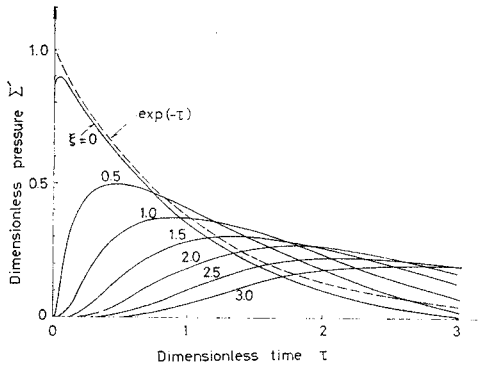

Fig. 4 Response of Voigt model subjected to a spike pulse.

As is known from the rheological mechanism Voigt model behaves as a perfectly rigid body at the instance of loading, so that wave front goes forwards in the medium with infinite velocity. There occurs no shock front at all, the duration time at each situation gradually increasing with increase in depth. Thus the wave form in Voigt material becomes flatter as the stress wave penetrates into the medium.

(2) Maxwell model

Substituting $\beta=1$ into Eq. (33), the numerical calculation has been performed just same as before. Thirty terms have been adopted for calculating the modified Bessel function at the right hand side of the equation, which is considered to be adequate for precision. The result is indicated in Fig. 5.

Comparing the figure with Fig. 4 for Voigt model, there exist remarkable differences as follows:

1) Maxwell model has a finite wave velocity; the wave front propagates in the medium with an elastic velocity $\sqrt{E/\rho}$.
2) There is a shock front even when the wave proceeds into greater depth and the peak stress occurs at the wave front.
3) Wave form at the boundary surface does not collapse as the wave goes down.

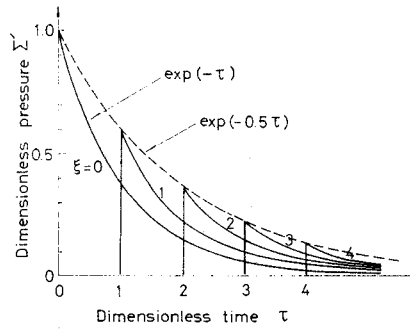

Fig. 5 Response of Maxwell model subjected to a spike pulse.

The attenuation of stress at the shock front acts on the first term of the right hand side in Eq. (33), which indicates that in spite of the wave form at the boundary surface the attenuation is uniquely expressed as $\exp(-0.5\tau)$ as shown in Fig. 5.

5. STANDARD LINEAR VISCOELASTIC MODEL

The result of calculation for Voigt and Maxwell model described in the preceding section explains to some extent the important response characters of clay indicated in the impact test. Precisely investigating, it can be recognized that the soil exhibits characteristics expressed by both models.

Performing the wave propagation test for clay, in fact, there exists few collapse of wave in the neighbourhood of the loading surface, whereas the wave does collapse its form as it penetrates deeper and deeper. To express such a behavior we take a standard linear viscoelastic model. The model is a true three-parameter model shown in Fig. 6, this having two springs and one dashpot. The constitutive equation of this model is written as:

$$E\varepsilon+\frac{1}{\mu}\varepsilon_t=\sigma\left(1+\frac{E}{E'}\right)+\frac{\sigma_t}{E'\mu} \quad \cdots\cdots\cdots\cdots(35)$$

Morrison[4] has obtained the following solution of

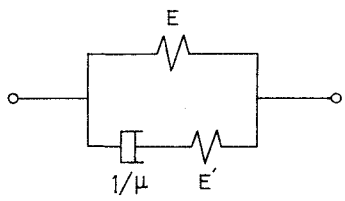

Fig. 6 Standard linear viscoelastic model.

one-dimensional wave propagation in this model, for the case of step-pulse type boundary stress.

$$\Sigma'(\xi,\tau)=\exp\left\{\frac{-\xi}{2(k)^{1/2}(k+1)^{3/2}}\right\}+\int_{\frac{(k)^{1/2}}{(k+1)^{3/2}}\xi}^{\tau}B(\xi,\zeta)\,d\zeta \quad \cdots\cdots(36)$$

where,

$$k=E/E',\quad \tau\geq\frac{(k)^{1/2}}{(k+1)^{3/2}}\xi$$

The functional form of $B(\xi,\zeta)$ is written in the literature[4], being very complex to replace here. It appears that Voigt and the standard linear viscoelastic models exhibit a very similar stress distribution for large times and this behavior will greatly differ from that of the elastic rod, due to viscous flow which has taken place. For shorter times the standard linear viscoelastic model would in this case also be better represented by Maxwell model if the material constants were chosen to give the same wave front velocity. According to Eq. (36), the stress wave propagates in the medium with a velocity of $\sqrt{(E+E')/\rho}$.

No analytical solution has been found regarding the response of this model to the spike-pulse type boundary stress. Only one way of approach using the characteristic line method has been tried by Lai and Sauer[6], giving an extensive numerical solution.

Here the authors propose another method of solution by using the principle of superposition, since the above-mentioned rheological models express in any case the linear viscoelasticity. In this method the surface stress of exponential decaying type is uniformly divided into ten step-pulse type stresses as shown in Fig. 7, and the solution by Eq. (36) for each step is finally superposed with each other.

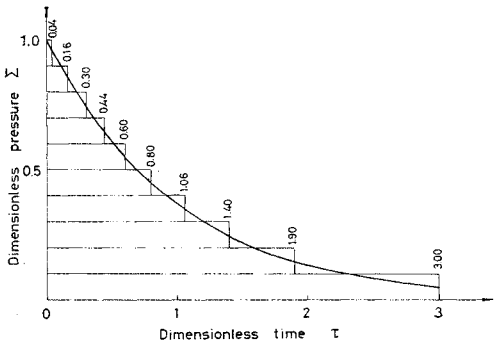

Fig. 7 Method of superposition.

In order to confirm the accuracy of this method of superposition the numerical calculation has been tried at first to Voigt and Maxwell models, to which the analytical solution was obtained for both boundary stresses for spike-pulse type and step-pulse one. The results are shown in Fig. 8 and Fig. 9, from which one can recognize that the division of

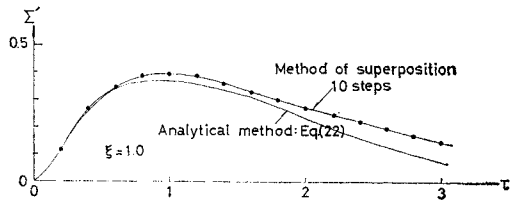

Fig. 8 Response of Voigt model subjected to a spike pulse ($\xi=1.0$).

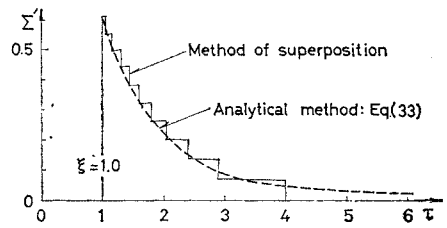

Fig. 9 Response of Maxwell model subjected to a spike pulse ($\xi=1.0$).

the boundary spike-pulse into ten step-pulses gives satisfactory accuracy for both cases. The extreme case of infinite number of division reaches the following Duhamel's integral :

$$x(t)=f(0)g(t)+\int_0^t f'(\tau)g(t-\tau)\,d\tau \quad \cdots\cdots(37)$$

where, $f(t)$ denotes the response function to the step-pulse type surface stress and $g(t)$ the function to the arbitrary stress.

Fig. 10 illustrates the behavior of stress propagation in the standard linear viscoelastic model obtained by means of the above-mentioned method of superposition. The parameter ratio is $k=1$, *i.e.*, $E=E'$. As is clear from the first term of the right hand side of Eq. (36), the stress attenuation at the shock front depends upon the parameter ratio k; for this example it decays in the manner of $\exp(-0.25\tau)$. As would be anticipated there exist discontinuous stress jumps in the neighbourhood of the surface where the value of ξ in Eq. (36) is small and, at the same time, there is no collapse of wave in these positions. Thus the medium behaves like a Maxwell body there. Reaching $\xi\geq 5.0$, however,

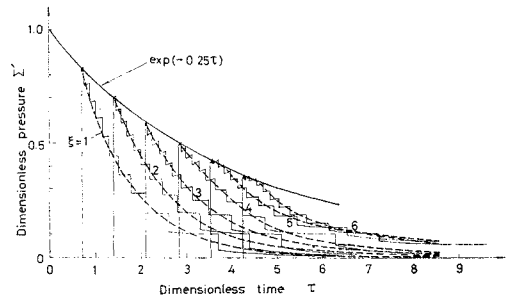

Fig. 10 Response of standard linear viscoelastic model subjected to a spike pulse ($k=1$).

there appears some roundness at the wave front and, for still larger value of ξ, the peak stress does not occur at the wave front, the collapse of wave form being much remarkable. It can be said, therefore, that the medium behaves like a Voigt body here.

Lai and Sauer[6] have called the depth at which this phenomenon appears as the critical depth and defined by the following equation :

$$\frac{z_{cr}}{c_0}=\frac{8}{1+4E/E'}\left(\frac{1}{E'\mu}\right)^2\frac{1}{p_0}\frac{dp}{dt}\Big|_{t=0} \quad \cdots\cdots(38)$$

where, $c_0=\sqrt{E'/\rho}$, p_0 denotes the peak value of the applied stress.

It can be seen that for any depth less than the corresponding critical depth, the compressive stress will initially decrease with time; and for any depth greater than the critical depth the stress will initially increase with time. Hence, for ξ less than ξ_{cr} (that is, the dimensionless representation of z_{cr}) the maximum response attenuates exponentially with depth, and for ξ greater than ξ_{cr} maxima occur which attenuate at a lesser rate, depending on the parameter ratio k/μ and on the overpressure wave form.

6. CONSIDERATION OF EXPERIMENTAL RESULTS

Some results obtained by the longitudinal impact stress propagation test for cohesive soil[8] are discussed here. In this test the clay specimen (6 cm in diameter and 60 cm in length) was suspended horizontally by some ribbons made of cloth attached to a rigid frame, and a falling weight struck the impact end of the specimen to generate a pulsative force. At each point of the specimen a very small pressure gauge was embedded to measure the pressure propagating through the specimen.

In this test the stress wave at the impact end is approximately given in the following form :

$$p(0,\ t)=p_0\ \mathrm{ext}(-\alpha t) \quad \cdots\cdots(39)$$

Assuming that the particle velocity behind the wave front is constant, the peak stress p_x at the arbitrary point is given as :

$$\frac{p_x}{p_0}=\frac{c}{\alpha x}\left\{1-\exp\left(\frac{\alpha x}{c}\right)\right\} \quad \cdots\cdots(40)$$

Thus it is known that the peak stress in the clay specimen attenuates with distance and the character depends upon the celerity c and the wave form of given pulsative stress. Fig. 11 is the comparison between the experimental results and Eq. (40), which shows that the attenuation of peak stress is considerably larger than the theoretical value deduced under the above-mentioned assumption without considering the viscous damping.

If we define the time for the pressure to take in decreasing its intensity to the peak pressure multiplied by $1/e$ ($=0.368$) from the instance of the impact as "the duration time of pressure wave", we obtain the following relationship, refering Fig. 12.

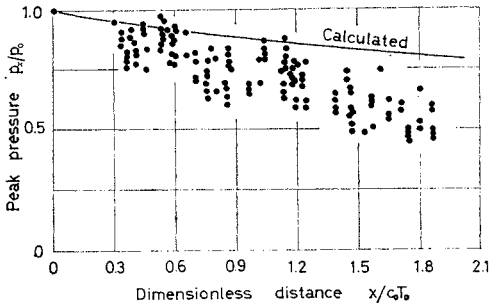

Fig. 11 Peak stress attenuation with distance.

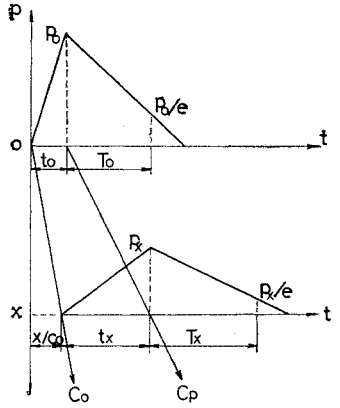

Fig. 12 Rise time and decay time at each point.

$$\frac{t_x+T_x}{t_0+T_0}=\frac{p_0}{p_x}=\frac{p_0 x}{c\int_0^t p(0,\ t)dt} \quad \cdots\cdots(41)$$

where $p(0,\ t)$ denotes the applied surface pressure.

For the duration time of the pressure wave, the comparison of the calculated results with the measured one is illustrated in Fig. 13. Both theoretically and experimentally the duration time increases with distance, and it may be found from Eq. (41) that the duration time enlarges for soft soil and for higher intensity of the peak pressure. As in Fig.

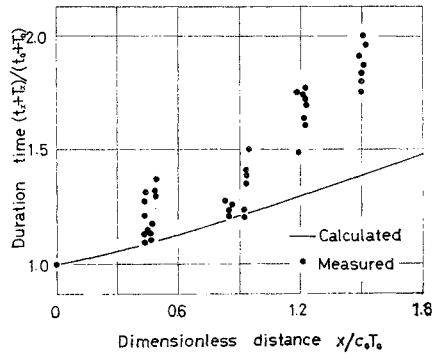

Fig. 13 Duration time increasing with distance.

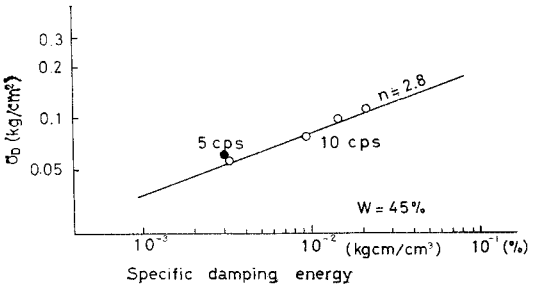

Fig. 14 Specific damping energy *vs.* maximum stress amplitude.

13 experimental results have fairly larger values than the calculated ones without considering the viscous damping of material.

It has also been found out from the longitudinal forced vibration test that the correlation between the maximum stress amplitude and the specific damping energy gives a straight line on a logarithmic paper with a slope of $n \fallingdotseq 2.8$ as indicated in Fig. 14[10]. This suggests that the damping of clay used in the experiment can be regarded approximately as the viscous damping[11].

7. CONCLUSION

In this paper are studied theoretical solutions for the one-dimensional stress propagation problems in the case of boundary stress forming a spike pulse with exponential decay. Theoretical models considered here are Voigt model, Maxwell model and the standard linear viscoelastic model with three parameters. For the latest there has not been any analytical solution except that for a step-pulse type boundary stress by Morrison *et al.* The authors have proposed a solution in the present study, using the principle of superposition. In this method the surface stress of exponential decaying type is uniformly divided into ten step-pulse type stresses, and the solution for each step is finally superposed with each other.

As the result, it is known that the standard linear viscoelastic model considerably well explains the wave propagation behaviors in saturated clay. The characteristics are that there exist discontinuous stress jumps in the neighbourhood of the surface of medium and, at the same time, there is no collapse of wave in these positions. Reaching deeper, there appears some roundness at the wave front and, at greater depths, the peak stress does not occur at the wave front, the collapse of wave form being much remarkable. Thus cohesive soils have both characteristics of Voigt and Maxwell bodies, and the standard linear viscoelastic model is valid for expressing a finite wave velocity through the soil medium.

REFERENCES

1) Krizek, R.J. and A.G. Franklin : Energy Dissipation in a Soft Clay, Proc. Intern. Symp. Wave Propagation and Dynamic Properties of Earth Materials, 1967, pp. 797-807.
2) Lee, E.H. and I. Kanter : Wave Propagation in Finite Rods of Viscoelastic Material, J. Appl. Phy., Vol. 24, 1953, pp. 1115-1122.
3) Glauz, R.D. and E.H. Lee : Transient Wave Analysis in a Linear Time-Dependent Material, J. Appl. Phy., Vol. 25, 1954, pp. 947-953.
4) Morrison, J.A. : Wave Propagation in Rods of Voigt Material and Visco-Elastic Materials with Three-Parameter Models, Q. Appl. Math., Vol. 14, 1956, pp. 153-169.
5) Lee, E.H. and J.A. Morrison : A Comparison of the Propagation of Longitudinal Waves in Rods of Viscoelastic Materials, J. Polymer Sci., Vol. 14, 1956, pp. 93-110.
6) Lai, W. and F.M. Sauer : Propagation of Stress Pulses in Standard Linear Viscoelastic Materials, Stanford Research Inst., SU-2917, DASA 1266-1, 1961, pp. 15-56.
7) Seaman, L. : One-Dimensional Stress Wave Propagation in Soils, Stanford Research Inst., AD-632106, DASA 1757, 1966, pp. 1-163.
8) Akai, K., M. Tokuda and T. Kiuchi : Experimental Study on the Propagation of Stress Wave in Cohesive Soils, Proc. JSCE, No. 161, 1969, pp. 59-67.
9) Akai, K. and M. Hori : Basic Study on the Dynamic Soil-Structure Interaction, Proc. JSCE, No. 173, 1970, pp. 61-78.
10) Akai, K. and Y. Yamauchi : Response Characteristics of Saturated Clay to Impact Loading, Soils and Foundations, Vol. 8, No. 2, 1968, pp. 13-34.
11) Akai, K. : Damping Characteristics of Saturated Clay Subjected to Impact or Vibration, Proc. 14th Japan Congr. Materials Research, 1971 (under printing).

APPENDIX Inversive Laplace Transformation

For $\beta=1$ Eq. (13) is written as

$$L\{\Sigma'(\xi,\tau)\}=\frac{1}{s+1}\exp\left\{\frac{-\xi s}{\sqrt{1+s}}\right\} \cdots\cdots\cdots (A\text{-}1)$$

The integral formula shows that if

$\bar{x}(s)=L\{x(t)\}$ and

$\phi(s)\exp\{-u\psi(s)\}=L\{K(t,u)\}$

then,

$$\phi(s)\bar{x}\{\psi(s)\}=L\left\{\int_0^\infty K(t,u)x(u)du\right\} \quad (A\text{-}2)$$

We use the following transform formulae :

(a) $\dfrac{1}{\sqrt{s}}\exp\{-\xi\sqrt{s}\}=L\left\{\dfrac{1}{\sqrt{\pi\tau}}\exp\left(-\dfrac{\xi^2}{4\tau}\right)\right\}$

(b) $\dfrac{1}{\sqrt{s}}\exp\left\{-\dfrac{\eta}{s}\right\}=L\left\{\dfrac{1}{\sqrt{\pi\tau}}\cos(2\sqrt{\eta\tau})\right\}$

(c) $\dfrac{1}{s^{3/2}}\exp\left\{-\dfrac{\eta}{s}\right\}=L\left\{\dfrac{1}{\sqrt{\pi\eta}}\sin(2\sqrt{\eta\tau})\right\}$

Substituting $\phi(s)=\dfrac{s-1}{s^{3/2}}$ and $\psi(s)=\left(\dfrac{s-1}{\sqrt{s}}\right)^2$ into (a),

$$\phi(s)\exp\{-u\psi(s)\}=\frac{s-1}{s^{3/2}}\exp\left\{-u\left(\frac{s-1}{\sqrt{s}}\right)^2\right\}$$
$$=\left(\frac{1}{\sqrt{s}}-\frac{1}{s^{3/2}}\right)\exp\left\{-u\left(s-2+\frac{1}{s}\right)\right\}$$

Using (b) and (c),

$$\phi(s)\bar{x}\{\psi(s)\}=\frac{s-1}{s^{3/2}}\times\frac{s^{1/2}}{s-1}\exp\left\{-u\left(\frac{s-1}{\sqrt{s}}\right)\right\}$$
$$=\frac{1}{s}\exp\left\{-u\left(\frac{s-1}{\sqrt{s}}\right)\right\}$$

Thus

$$\frac{1}{\sqrt{s}}\exp\left\{-\eta\left(s-2+\frac{1}{s}\right)\right\}$$
$$=L\left\{\frac{\cos(2\sqrt{\eta}\sqrt{\tau-\eta})}{\sqrt{\pi}\sqrt{\tau-\eta}}\exp(2\eta)H(\tau-\eta)\right\}$$
.....(A-3)

$$\frac{1}{s^{3/2}}\exp\left\{-\eta\left(s-2+\frac{1}{s}\right)\right\}$$
$$=L\left\{\frac{\sin(2\sqrt{\eta}\sqrt{\tau-\eta})}{\sqrt{\pi}\sqrt{\eta}}\exp(2\eta)H(\tau-\eta)\right\}$$
.....(A-4)

Then, using the integral formula (A-2) for $s>1$,

$$\frac{1}{s}\exp\left\{-\frac{\xi(s-1)}{\sqrt{s}}\right\}$$
$$=L\left\{\frac{1}{\pi}\int_0^\tau\frac{\cos(2\sqrt{\eta}\sqrt{\tau-\eta})}{\sqrt{\eta}\sqrt{\tau-\eta}}\exp\left(2\eta-\frac{\xi^2}{4\eta}\right)d\eta\right\}$$
$$-L\left\{\frac{1}{\pi}\int_0^\tau\frac{\sin(2\sqrt{\eta}\sqrt{\tau-\eta})}{\eta}\exp\left(2\eta-\frac{\xi^2}{4\eta}\right)d\eta\right\}$$
.....(A-5)

Therefore, one obtains the inversive transformation of Eq. (A-1) :

$$\Sigma'(\xi,\tau)=\frac{e^{-\tau}}{\pi}\int_0^\tau\left[\frac{\cos\{2\sqrt{\eta(\tau-\eta)}\}}{\sqrt{\eta(\tau-\eta)}}\right.$$
$$\left.-\frac{\sin\{2\sqrt{\eta(\tau-\eta)}\}}{\eta}\right]\exp\left(2\eta-\frac{\xi^2}{4\eta}\right)d\eta$$
.....(22)

(Received Aug. 19, 1970)

昭和三十七年五月二十八日　印刷
昭和四十六年一月十五日　発行
昭和四十六年一月二十日　第三種郵便物認可
（毎月一回二十日発行）

土木学会論文報集　第185号

定価三〇〇円